

Short Communication

Prediction of Wear Resistance of Ultrasonic Electrodeposited Ni-SiC Nanocoatings using BP-NN Model

Hui Wang¹, Weipeng Yu¹, Haijun Liu^{1*}, Qiang Li², Fafeng Xia², Chunyang Ma²

¹ College of Engineering and Technology, Jiyang College of Zhejiang Agriculture & Forestry University, Zhuji, 311800, China;

² College of Mechanical Science and Engineering, Northeast Petroleum University, Daqing 163318, China

*E-mail: chunyangandma@163.com, 20180050@zafu.edu.cn (H. Liu)

Received: 15 November 2020 / Accepted: 26 January 2021 / Published: 28 February 2021

This paper adopts neural network technology to construct a BP-NN (Back-propagation neural network) model with 3×8×1 structure, and the model was used to predict the wear resistance of ultrasonically electrodeposited Ni-SiC nanocoating. The impact of plating parameters on composition and microstructure of the Ni-SiC nanocoatings were investigated by scanning electron microscopy (SEM), atomic force microscopy (AFM), and X-ray diffraction (XRD) and wear testing. The results indicated that when the number of hidden layers and neurons of the BP-NN model are 1 and 8, respectively, and the root mean square error of the BP-NN model was minimal with a value of 1.24%. The prediction value of the BP-NN model was not much different from the experimental value, and the maximum error obtained was 1.51%. When the concentration of SiC particles was taken as 8 g/L, current density was maintained at 2 A/dm², and the temperature was kept at 40°C, the SiC particles were uniformly distributed in the Ni-SiC nanocoating, and the nickel grains of the coating were significantly refined, as indicated by the diffraction peaks of the nickel grains which became wider and shorter.

Keywords: Ni-SiC nanocoating; BP-NN model; microstructure; wear; prediction

1. INTRODUCTION

Over the past few decades, Ni-SiC nanocoatings have been widely used in the mechanical, petroleum, aviation, medical, chemical, and military fields due to their excellent material properties such as wear resistance, corrosion resistance, high-temperature oxidation resistance, and high hardness [1-6]. In general, ultrasonic-assisted electrodeposition technique is a simple method with high electrodeposition efficiency and low energy consumption to prepare nanocoatings [7-12]. Cai *et al.* [13]

reported the preparation of Ni-SiC composite nanocoatings via ultrasonic-assisted electrodeposition. The results indicated that ultrasonic waves could improve the electrodeposition efficiency and the structure of the nanocoating. Under the synergistic action of ultrasonic wave and electrodeposition, the nanocoating in the combination of Ni matrix and SiC nanoparticles, enhanced the mechanical and electrochemical properties substantially, and the material has shown excellent electrical conductivity and stable structure. Ma *et al.* [14] have reported the preparation of Ni-SiC nanocoating via an electrodeposition method assisted by ultrasonic treatment. The results indicated that the Ni-SiC nanocoating prepared by ultrasonic-assisted electrodeposition method has better specific capacitance.

Back-propagation neural network (BP-NN) models are a kind of artificial neural network model which can establish complex nonlinear relationship between forward data propagation and reverse error transmission. Recently, there are various reports where this model has been applied to predict the performance of nanocoatings [15-17]. Xu [18] adopted BP-NN model to predict the corrosion behavior of pulse electrodeposition of Ni-TiN nanocoating. The results indicated that the BP-NN model could be successfully utilized to predict the relative error of corrosion weight loss of Ni-TiN nanocoating, and the maximum mean square error obtained was only 9.8%. Lu [19] adopted BP-NN to simulate and predict designed parameters of the Cu-Al₂O₃ nanocoating prepared by electrodeposition. The result revealed that the Al₂O₃ particles were uniformly distributed in the copper layer, and the particle content can reach up to 14.43%.

Although many reports on ultrasonic-assisted electrodeposition of metal matrix composites, few investigations are available concerning the detailed forecast on the wear resistance of ultrasonically electrodeposited Ni-SiC nanocoating. Based on the above discussion, Ni-SiC nanocoatings were obtained by ultrasonic electrodeposition method, and their wear resistance was tested and analyzed by an UMT-2 type friction and wear tester. In addition, the microstructure and composition of Ni-SiC nanocoatings were investigated through scanning electron microscopy (SEM), atomic force microscopy (AFM) and X-ray diffraction (XRD) methods. Finally, the wear resistance of the nanocoatings was predicted through a BP-NN model.

2. EXPERIMENTAL

2.1 Deposition of Ni-SiC nanocoating

In this study, Ni-SiC nanocoatings were deposited on 40Cr steel via ultrasonic electrodeposition. The composition and preparation process of composite plating solution are presented in Table 1. The 40Cr steel (dimension 30 × 20 × 10 mm) was used as cathode and pure nickel plate (99% purity) was used as anode. The electrode gap was kept at 25 mm. Prior to electroplating, the 40Cr steel substrate was first polished by metallographic sandpaper with 0.1-0.15 μm of surface roughness. It was followed by ultrasonic cleaning in absolute ethyl alcohol with the ultrasonic power of 150 W for 20 min, and washed with distilled water at 25°C. Fig. 1 represents the diagram of the electrodeposition device of Ni-SiC nanocoating. The device is composed of a pulse power box, a heating apparatus and the ultrasonic generator. The pulse current was produced by a pulse power box (DS1102U, from Suzhou Diancheng

2.2 Characterization

The wear test of Ni-SiC nanocoating was performed using UMT-2 type friction and wear tester. The wear mass measurement of coating specimen was done by 0.1 mg AUW-220 type electronic analytical balance. The surface morphologies, microstructure and composition of ultrasonic electrodeposited Ni-SiC nanocoatings were investigated by SEM (S3400), XRD (XRD-6000) and Nanoscope IIIa atomic force microscopy (AFM). In addition, friction wheel was utilized on nanocoating exterior under 8 N infliction load and 0.2 m/s uniform speed under oil lubrication at room temperature to determine rolling resistance. A schematic diagram of measuring equipment of wear properties is displayed in Fig. 2. SEM was used to determine the the wear surface morphology of Ni-SiC nanocoating after 25 min of wear. In addition, a CS450 electrochemical workstation was used to measure corrosion behaviors of the nanocoatings in 3.5 wt.% NaCl solutions.

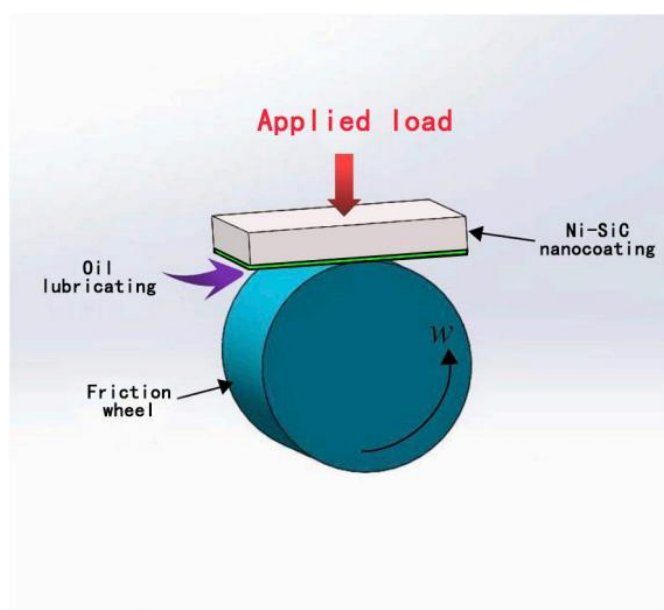


Figure 2. Schematic diagram of the experiment for measuring the wear properties of the Ni-SiC nanocoatings.

2.3 BP-NN model

BP-NN model is an information processing system based on simulating the structure and function of the brain neural network. It is comprised of simple artificial nodes and can simulate biological nerves with mathematical model. In addition, BP-NN model is a tool that can deal with nonlinear systems effectively because of its characteristics of self-learning, self-organization, adaptation, nonlinear function approximation, and strong fault tolerance, and it can realize the fuzzy control, prediction on image recognition, and the functions of simulation.

In this work, BP-NN model has been utilized to study the wear mass loss of Ni-SiC nanocoating. The BP-NN model consists of input layer, output layer and conceal layer. In this paper, the SiC particle concentration (X_1), current density (X_2) and temperature (X_3) have been taken as the input layer, the

wear amount (Y) of the Ni-SiC nanocoating has been taken as the output layer of the BP-NN model (see Fig. 3). When modeling the BP-NN, Sigmoid function is used in the implicit layer of neural network because of its good generality, good training effect and small calculation error and its calculation formula is given as:

$$f(x) = \frac{1}{1 + e^{-x}} \quad (1)$$

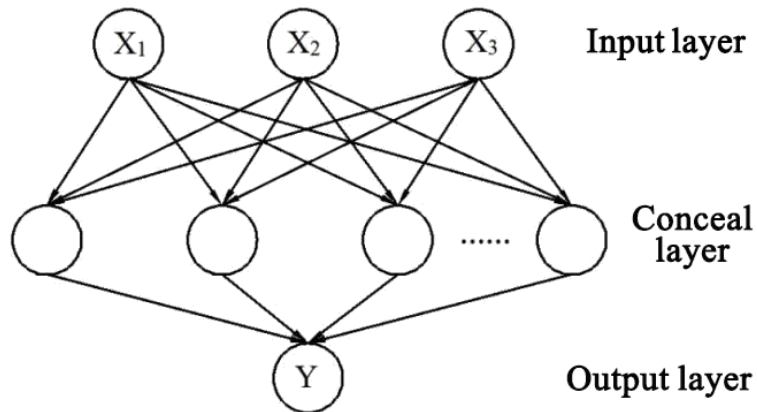


Figure 3. Schematic of the BP-NN model.

3. RESULTS AND DISCUSSION

3.1 BP-NN model training

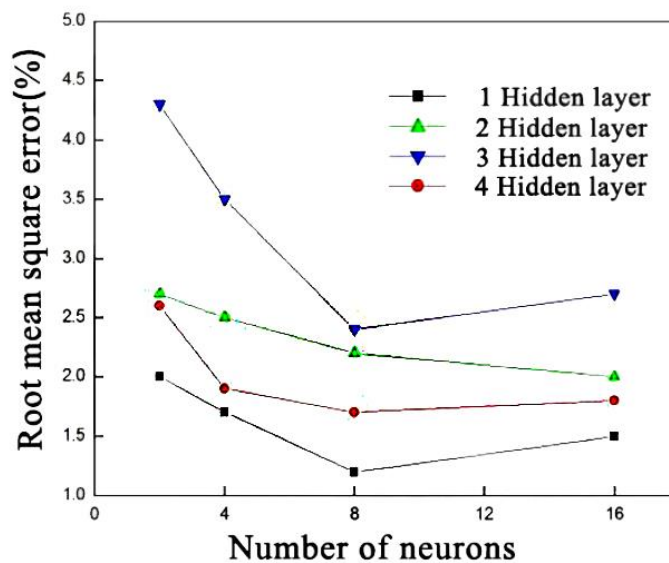


Figure 4. Influence of different number of neurons and hidden layer on the root mean square error of BP-NN model.

To check the prediction accuracy of the BP-NN model, performance evaluation is carried out which includes finding the coefficient of correlation and determination of error between actual experimental values and predicted values. Fig. 4 presents the influence of the number of neurons and the number of hidden layers on the root mean square error of the BP-NN model. If the number of hidden layers and the number of neurons were 1 and 8, respectively, the root mean square error of the BP-NN model has been found to be the smallest, and its minimum value obtained is 1.24%. Therefore, the BP-NN model of $3 \times 8 \times 1$ structure was used to predict the wear resistance of Ni-SiC nanocoating. The fitting similarity of the BP-NN model has been obtained as $R=0.9992$.

3.2 BP-NN prediction

Taking 1~20 groups of data in Table 2 as training samples, the BP-NN model with 3×8 and 1 structure was used to build a prediction model of wear resistance of Ni-SiC nanocoating based on BP-NN. Fig. 6 shows the prediction results of the model on the wear performance of nanocoating. The BP-NN model was established, and the last 10 groups of data in Table 2 are selected as test samples to predict and analyze the wear of ultrasonically electrodeposited Ni-SiC nanocoating, to verify the reliability of the BP-NN model. The prediction results indicated the maximum relative error between the predicted values and the experimental values of the BP-NN model has been found to be 1.51%. The results are similar to the work described by Xu et al. [20].

Table 2. Input parameters and experimental wear value.

Serial number	SiC particle concentration (g/L)	Current density (A/dm ²)	Temperature (°C)	Experimental wear value (mg)
1	2	0.5	20	13.42
2	4	1	30	10.56
3	6	1.5	40	11.32
4	8	2	50	10.78
5	10	2.5	60	12.43
.....				
47	2	2.5	60	11.01
48	4	2	50	12.21
49	8	1	30	8.63
50	10	0.5	20	20.74

3.3 Coating characterization

Fig. 5 presents the SEM image of ultrasonically electrodeposited Ni-SiC nanocoating under different process parameters.

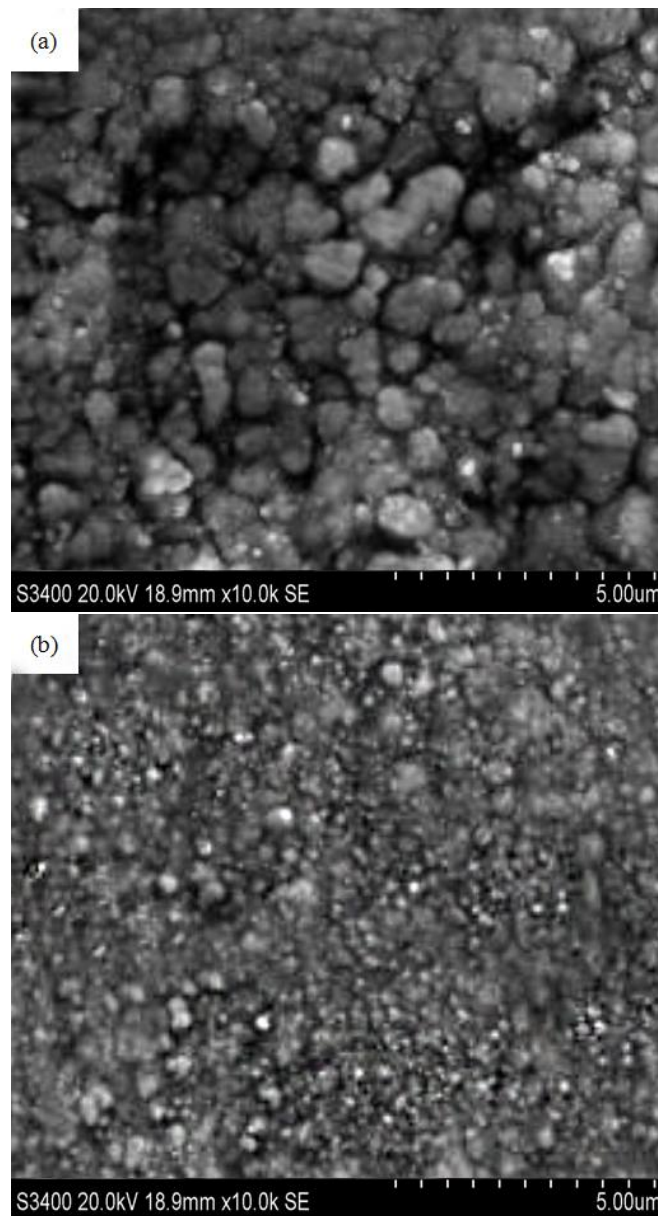


Figure 5. Surface morphologies of Ni-SiC nanocoatings observed by SEM: (a) SiC particle concentration 4 g/L, current density 1 A/dm², ultrasonic power 150 W, electroplating time 45 min, temperature 20 °C, (b) SiC particle concentration 8 g/L, current density 2 A/dm², ultrasonic power 150 W, electroplating time 45 min, temperature 40 °C.

When the concentration of SiC particles was utilized as 4 g/L and the current density was maintained at 1 A/dm², at 20°C, the surface of Ni-SiC nanocoating fluctuates greatly and the nickel grain size was found to be coarse. Moreover, the agglomeration of SiC particles on the coating surface (white particles in Fig. 5a) was evident from the SEM image, and the distribution of SiC particles on the coating surface remained irregular. When the SiC particle concentration was taken as 8 g/L, the current density was maintained at 2 A/dm², at 40°C, the SiC particles are uniformly distributed on the Ni-SiC nanocoating, and the nickel grains of the coating has been found to be significantly refined. This result is fundamentally the same as the found depicted by Sun *et al.* [21].

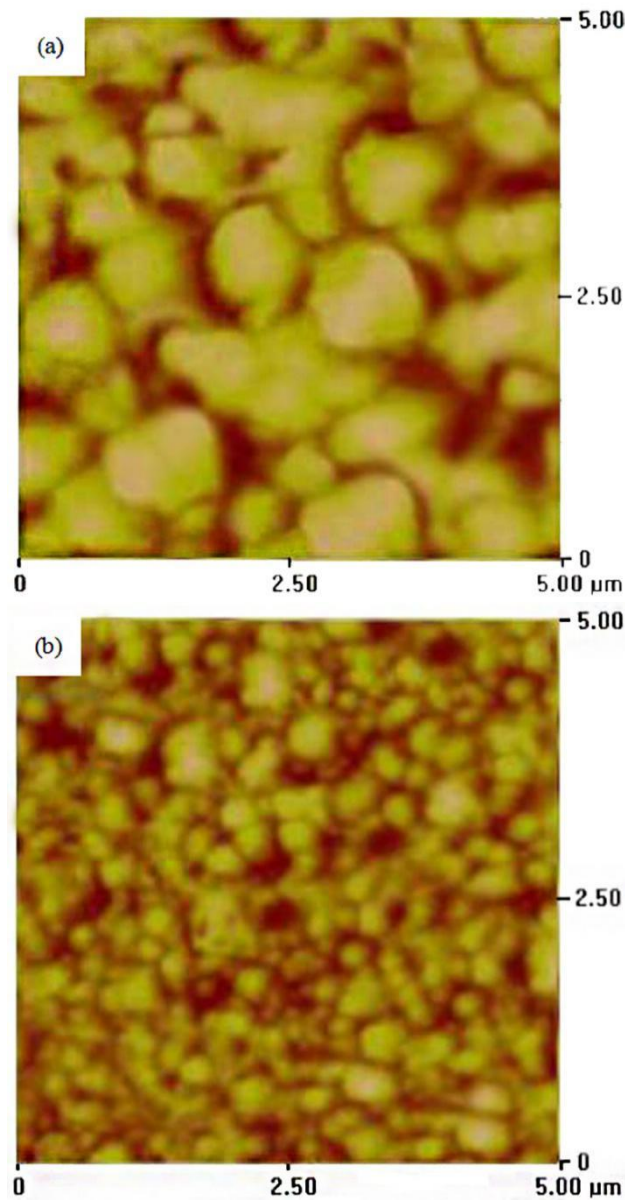


Figure 6. Surface morphologies of Ni-SiC nanocoatings observed by AFM: (a) SiC particle concentration 4 g/L, current density 1 A/dm², ultrasonic power 150 W, electroplating time 45 min, temperature 20 °C, (b) SiC particle concentration 8 g/L, current density 2 A/dm², ultrasonic power 150 W, electroplating time 45 min, temperature 40 °C.

Fig. 6 presents the AFM image of ultrasonic electrodeposition of Ni-SiC nanocoating under different process parameters, when SiC particle concentration was utilized at 4 g/L, and current density was maintained at 1 A/dm², at 20 °C, the surface of Ni-SiC nanocoating layer fluctuates greatly, the grain size obtained was thicker and the structure remained irregular. When SiC particle concentration was maintained at 8 g/L, and current density was utilized of 2 A/dm², at 40 °C, the Ni-SiC nanocoating obtained was flat and the nickel particles deposited were fine.

The Ni-SiC nanocoating prepared by ultrasonic electrodeposition under different technological parameters was mapped by X-ray diffraction. The diffraction pattern is presented in Fig. 7. The different

process parameters have great influence on the XRD spectrograms of Ni-SiC nanocoating. When the SiC particle concentration was taken as 4 g/L, current density was maintained at 1 A/dm, at 20°C, the diffraction peak of nickel grain in Ni-SiC nanocoating was fine and high, which indicates that the nickel grain in this coating was coarse. When SiC particle concentration was taken as 8 g/L, current density was maintained at 2 A/dm², at 40°C, the diffraction peak of nickel grain in Ni-SiC nanocoating becomes wider and shorter indicating that the nickel grain in the nanocoating is much more refined under that condition. XRD diffraction patterns also illustrate the presence of Ni and SiC phases in ultrasonic electrodeposition of Ni-SiC nanocoatings. This result is consistent with that reported by Xia *et al.* [22].

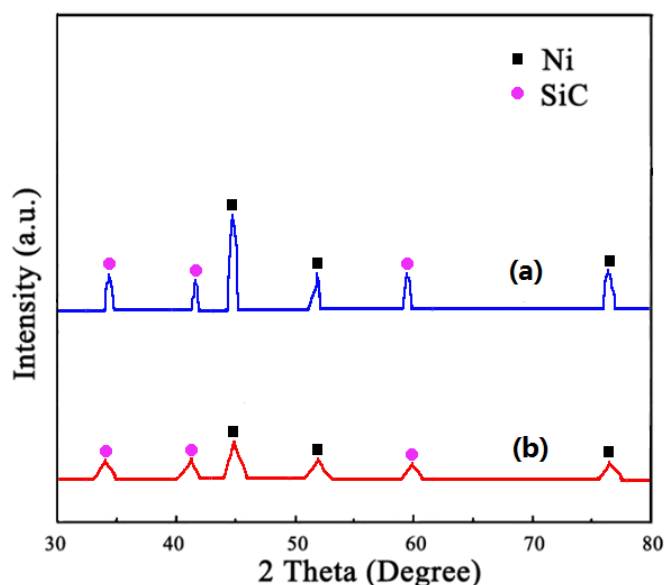


Figure 7. XRD spectrograms of Ni-SiC nanocoatings obtained with different parameters: (a) SiC particle concentration 4 g/L, current density 1 A/dm², ultrasonic power 150 W, electroplating time 45 min, temperature 20°C, (b) SiC particle concentration 8 g/L, current density 2 A/dm², ultrasonic power 150 W, electroplating time 45 min, temperature 40°C.

The above observations can be explained as that when the concentration of SiC particles are relatively low, the probability of contact collision between SiC particles and cathode are small. As the particle concentration of SiC in the bath increases, the amount of SiC particles moving to the cathode surface increases per unit time. SiC particles can inhibit the growth of nickel grains, so the nickel grains in Ni-SiC nanocoating layer remains fine and smooth [23]. When the current density is small, the electric field force remains weak, and the deposition rate of SiC particles and nickel ions are slow, which makes the encapsulation ability of nickel particles to SiC particles poor, and hence the content of SiC particles in the Ni-SiC nanocoating found to be low. As the current density increases, the electric field force increases, and the content of SiC particles deposited in the coating increases, which results in the formation of the nanocoating layer and the fine particles. Furthermore, when low temperature is maintained, the bath solubility remains low and the electrochemical reaction rate is relatively slower.

With the increase of temperature, the solubility of the bath increases, and the conductivity increases, which increases the deposition rate of SiC particles and the recombination of SiC particles in the coating, so the nickel grains in the Ni-SiC nanocoating found to be fine.

3.4 Wear behavior assessment

Fig. 8 presents the friction coefficient curves of Ni-SiC nanocoatings prepared under different deposition parameters. The slopes of the friction coefficient curve of the Ni-SiC nanocoatings increased rapidly in the short sliding distance, and the curve tended to stabilize at a certain values until the end of the wear test. The average friction coefficient of Ni-SiC nanocoating prepared with SiC particle concentration of 4 g/L, current density of 1 A/dm² and temperature of 20°C was the smallest, while the mean friction coefficient found to be approximately 0.58. Among the main factors affecting the friction coefficient of Ni-SiC nanocoatings are the content and microhardness of SiC nanoparticles [24]. Therefore, the wear resistance was definitely improved through the well dispersion of SiC nanoparticles in Ni-SiC nanocoatings.

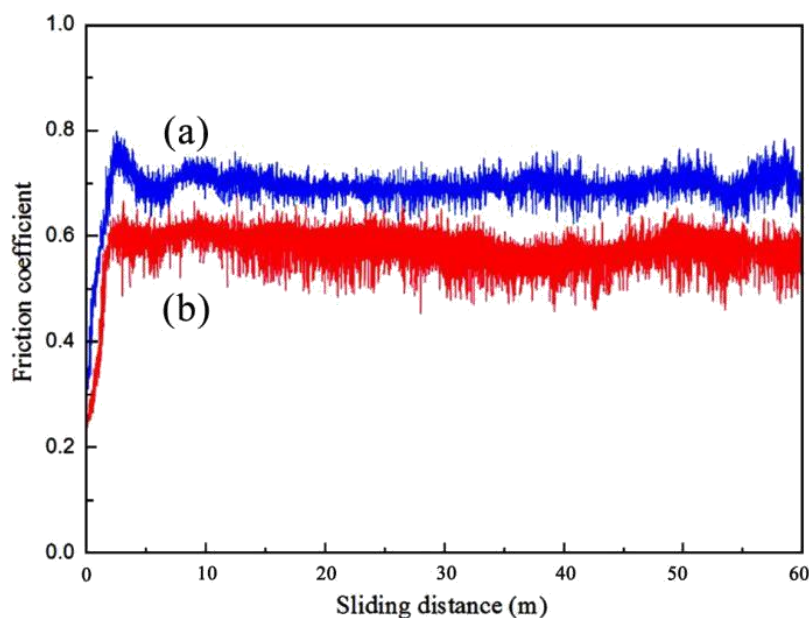


Figure 8. Friction coefficients of Ni-SiC nanocoatings obtained with different parameters: (a) SiC particle concentration 4 g/L, current density 1 A/dm², ultrasonic power 150 W, electroplating time 45 min, temperature 20°C, (b) SiC particle concentration 8 g/L, current density 2 A/dm², ultrasonic power 150 W, electroplating time 45 min, temperature 40°C.

Fig. 9 presents abrasion surface morphology of Ni-SiC nanocoatings deposited under different parameters. There were large deep grooves on the worn surfaces of Ni-SiC nanocoating deposited at SiC particle concentration of 4 g/L, the current density of 1 A/dm², at 20°C. It indicates that the Ni-SiC nanocoating surface is in a serious state of wear (Fig. 9a). Through comparison, the worn surface

morphology of nanocoating deposited at the SiC particle concentration of 8 g/L, current density of 2 A/dm² and temperature of 40°C was well distributed, while only a small number of low size scratches appeared on the surface, thus exhibiting the best wear resistance in this wear test (Fig. 9b). This result is consistent with the report explained by Zhang *et al.* [25].

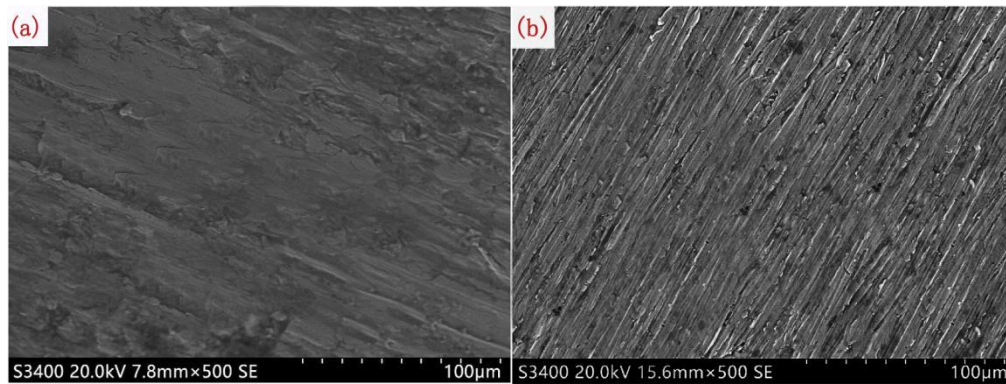


Figure 9. SEM images of the worn surface of Ni-SiC nanocoatings obtained with different parameters: (a) SiC particle concentration 4 g/L, current density 1 A/dm², ultrasonic power 150 W, electroplating time 45 min, temperature 20°C, (b) SiC particle concentration 8 g/L, current density 2 A/dm², ultrasonic power 150 W, electroplating time 45 min, temperature 40°C.

3.5 Corrosion behavior assessment

The Nyquist diagrams of Ni-SiC nanocoatings obtained at different plating parameters are presented in Fig. 10. The lowest impedance was discovered for the Ni-SiC nanocoating deposited at SiC particle concentration 4 g/L, current density 1 A/dm², ultrasonic power 150 W, electroplating time 45 min, and temperature 20°C. The result indicates that this nanocoating processes the worst corrosion resistance. However, the Ni-SiC nanocoating obtained at SiC particle concentration 8 g/L, current density 2 A/dm², ultrasonic power 150 W, electroplating time 45 min, and temperature 40°C has the the highest impedance, testifying the best corrosion resistance. The outcome is consistent with the study investigated by Ma *et al.* [26].

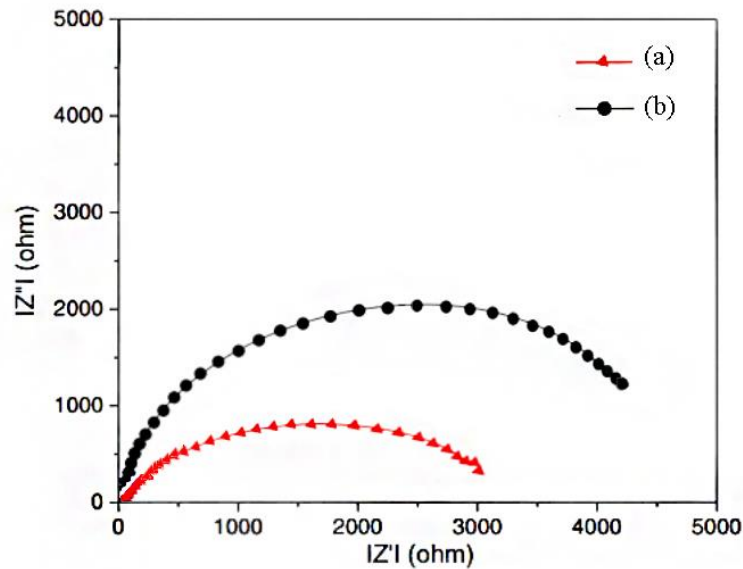


Figure 10. Nyquist curves of Ni-SiC nanocoatings obtained with different parameters: (a) SiC particle concentration 4 g/L, current density 1 A/dm², ultrasonic power 150 W, electroplating time 45 min, temperature 20 °C, (b) SiC particle concentration 8 g/L, current density 2 A/dm², ultrasonic power 150 W, electroplating time 45 min, temperature 40 °C.

4. CONCLUSION

(1) The BP-NN model with 3×8×1 structure is established. The model takes SiC particle concentration, current density and temperature as the input layer, and the wear amount of Ni-SiC nanocoating as the output layer. If the number of concealed layers and number of neurons are taken as 1 and 8, respectively, the root mean square error of the BP-NN model was found to be the smallest, and its minimum value obtained was 1.24%. BP prediction values of the neural network model were not much different from the experimental values, and the maximum error found was 1.51%.

(2) When the concentration of SiC particles was taken as 8 g/L, the current density was maintained at 2 A/dm², at 40 °C, the SiC particles were uniformly distributed in the Ni-SiC nanocoating, and the nickel grains of the coating are significantly refined.

(3) In the above mentioned condition the diffraction peak of nickel grain in Ni-SiC nanocoating becomes wider and shorter, which indicates that the nickel grain in the nanocoating was obviously refined under such parameters. In the same condition, the Ni-SiC nanocoating showed the lowest friction coefficient, smooth wear surface and only a low-sized scratches, with best wear resistance.

ACKNOWLEDGEMENT

This work has been supported by the National Natural Science Foundation of China (Granted no. 51974089) and the Talent Startup Project of Jiyang College of Zhejiang Agriculture and Forestry University (Granted nos. 03251700016 and 03251700017).

References

1. C. Ma, D. Zhao, W. Liu, F. Xia, P. Jin, and C. Sun, *Ceram. Int.*, 46 (11) (2020) 17631.
2. R. Ji, K. Han, H. Jin, X. Li, Y. Liu, S. Liu, T. Dong, B. Cai, and W. Cheng, *J. Manuf. Process.*, 57 (2020) 787.
3. H.Z. Zhou, W.H. Wang, Y.Q. Gu, X.X. Fang, and Y.Q. Bai, *Strength. Mater+*, 49 (1) (2017) 101.
4. Z. Zhang, and Q. Du, *J. Func. Mater.*, 50 (3) (2019) 3081. (in Chinese)
5. S. Dehgahi, R. Amini, and M. Alizadeh, *J. Alloys. Compd.*, 692 (2017) 622.
6. V.N. Tseluikin, and Y.Y. Kupriyanov, *Russ. J. Appl. Chem.*, 88 (12) (2015) 2074.
7. Y. Wang, Z. Liang, X. Zhou, and H. Jin, *Int. J. Electrochem. Sci.*, 13 (2018) 9183.
8. Y. Zhong, N. Guo, Z. Huang, L. Nie, and Y. Li, *Adv. Mat. Res.*, 154 (2011) 763.
9. C.A. León-Patiño, J. García-Guerra, E.A. Aguilar-Reyes, *Wear*, 426 (2019) 330.
10. M.Q. Guo, H.S. Hong, X.N. Tang, H.D. Fang, and X.H. Xu, *Electrochim. Acta.*, 63 (2012) 1.
11. H. Zhang, N. Zhang, and F. Fang, *Ultrason. Sonochem.*, 62 (2020) 104858.
12. F. Xia, J. Tian, W. Wang, and Y. He, *Ceram. Int.*, 42 (11) (2016) 13268.
13. C. Cai, X.B. Zhu, G.Q. Zheng, Y.N. Yun, X.Q. Huang, J.F. Yang, and Z. Zhang, *Surf. Coat. Technol.*, 205 (11) (2011) 3448.
14. C. Ma, G. Liang, Y. Zhu, H. Mu, and F. Xia, *Ceram. Int.*, 40 (2) (2014) 3341.
15. X. Peng, X. Xu, and J. Wang, *Ceram. Int.*, 44 (7) (2018) 8599.
16. M. Jiang, C. Ma, F. Xia, and Y. Zhang, *Surf. Coat. Tech.*, 286 (2016) 191.
17. D. Guo, Y. Han, C. Ma, W. Yu, F. Xia, M. Jiang, and X. Xu, *Surf. Rev. Lett.*, 26 (3) (2019) 10428.
18. Y. Xu, *Ordinance. Mater. Sci. Eng.*, 41 (6) (2018) 49. (in Chinese)
19. W. Lu, *Electroplat. & Pollut. Control.*, 28 (1) (2008) 20. (in Chinese)
20. Y. Xu, Y. Zhu, G. Xiao, and C. Ma, *Ceram Int.*, 40 (4) (2014) 5425.
21. C. Sun, X. Liu, C. Zhou, C. Wang, and H. Cao, *Ceram. Int.*, 45(1) (2019) 1348.
22. F. Xia, Q. Li, C. Ma, and X. Guo, *Ceram. Int.*, 46 (2) (2020) 2500.
23. F. Xia, W. Jia, C. Ma, and J. Wang, *Ceram Int.*, 44 (1) (2018) 766.
24. L. Benea, F. Wenger, P. Ponthiaux, and J.P. Celis, *Wear*, 266 (3) (2009) 398.
25. J. Zhang, J. Lei, Z. Gu, F. Tantai, and Y. Fang, *Surf. Coat. Tech.*, 393 (2020) 125807.
26. C. Ma, M. Jiang, and F. Xia, *Surf. Rev. Lett.*, 24 (2016) 17500631.